

Failure process of acrylic polyurethane coating under alternate wetting and drying condition

Yu Zuo, Liang Zhang, Xuhui Zhao, Yuming Tang, Xiaofeng Zhang

Beijing Key Laboratory of Electrochemical Process and Technology for Materials, School of Materials Science and Engineering, Beijing University of Chemical Technology, Beijing 100029, People's Republic of China
Correspondence to: X. Zhao (E-mail: xzhao@mail.buct.edu.cn)

ABSTRACT: The failure process of an acrylic polyurethane coating in simulated sea water under a wet-dry cyclic condition and immersion condition was studied with the methods of electrochemical impedance spectroscopy (EIS), Fourier transform infrared spectroscopy (FT-IR), and scanning electron microscope (SEM). The results show that the failure rate of acrylic polyurethane coating under the condition of wet-dry alternation is obviously greater than that under complete immersion. Under wet-dry condition, both the porosity and the water absorptivity of the coating are also greater than those under complete immersion condition. Owing to the physical effect of wet-dry alternation, the fillers in the coating surface layer may fall off and result in micro-pores, which could multiply the defects in the coating and accelerate the coating degradation. FT-IR analysis shows that the isocyanate group in the coating not only participates in the curing of coating, but also hydrolyzes with water molecule. The C-O bonds fracture partly due to hydrolysis of the main molecule chains, which is one reason of the coating failure. The failure process for acrylic polyurethane coating under a wet-dry cyclic condition is discussed. © 2015 Wiley Periodicals, Inc. *J. Appl. Polym. Sci.* **2015**, *132*, 41989.

KEYWORDS: ageing; coatings; characterization; degradation; electrochemistry; properties

Received 9 September 2014; accepted 16 January 2015

DOI: 10.1002/app.41989

INTRODUCTION

Organic coatings are widely used to protect steels from corrosion in marine environments. Under service conditions, the continuous migration of water, oxygen, ions, and aggressive species to coating/metal interface will lead to polymeric material degradation, coating delamination, and undercoating corrosion, and eventually cause the loss of corrosion protective function of organic coatings.^{1–3} Various studies^{2–8} have investigated the failure behavior of organic coatings and revealed that the water absorbability of the coatings may be one of the most important factors in undercoating corrosion. But these researches are mainly focused on the failure behavior of organic coatings under complete immersion or non-immersion. However, in fact, for the coatings used for marine engineering structures such as ship coatings, the areas of the coatings around the waterline experience alternate wetting and drying condition, and usually suffer more severe damages than those under complete immersion or non-immersion. Park⁹ monitored the water uptake of epoxy and polyurethane double coatings using electrochemical impedance spectroscopy (EIS), and discussed the mechanism of corrosion beneath organic coatings under cyclic wet-dry exposure in chloride-containing environments. Coniglio¹⁰ studied water sorption in 100% solids epoxy coatings

by the gravimetric liquid sorption measurements, and pointed out that alternating sorption-desorption cycles can increase the speed of water movement. Zhao¹¹ studied the deterioration process of the organic coating on carbon steel surface under cyclic wet-dry conditions, using electrochemical impedance spectroscopy (EIS) assisted by self-organizing feature map (SOM) network. Lendvay-Gyorik¹² studied the failure process of waterborne paint coatings such as styrene-acrylate and alkyd-acrylate coatings, found that the changing wet-and-dry environment improved their corrosion protection properties, and pointed out that water uptake and release removed the water-soluble components from the film and thereby contributed to the corrosion protection feature. Allahar¹³ studied the degradation behavior of an epoxy coating on an AA 2024-T3 substrate under cyclic dilute NaCl wetting and ionic liquid drying conditions. Wang¹⁴ studied on the deterioration process of organic coatings (iron red alkyd primer) under immersion and different cyclic wet-dry ratios by EIS, and pointed out that comparing with the immersed, the 4-4 h wet-dry cycles greatly accelerated the entire deterioration process, and the 12-12 h wet-dry cycles decelerated the entire deterioration process. However, compared with the studies on coating failure during immersion, the studies on the failure process of coatings under alternate wetting and drying

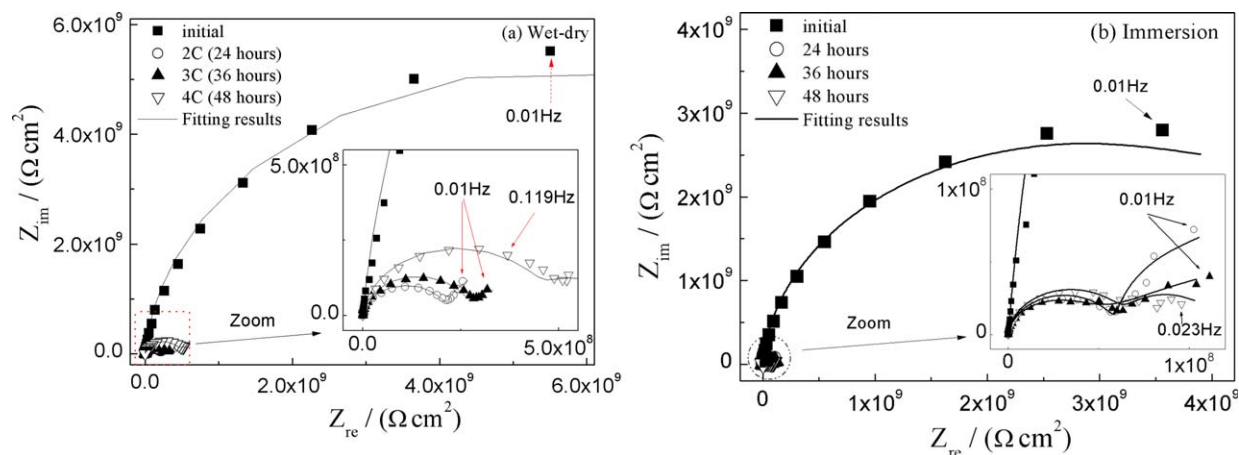


Figure 1. Nyquist plots of the coating samples under difference conditions (2–4 cycles) (a) wet-dry alternation and (b) immersion. [Color figure can be viewed in the online issue, which is available at wileyonlinelibrary.com.]

conditions are still very few, and the failure mechanism of coatings and underlying metal corrosion under wet-dry cycles is not very clear. Acrylic polyurethane coating is widely used as top coating for marine engineering structures due to its good weather resistance and appearance. In this work, under a wet-dry cyclic condition, the failure process of an acrylic polyurethane coating is studied by EIS and the failure mechanism is discussed with help of SEM and FT-IR analysis.

EXPERIMENTAL

Materials and Preparation of Specimens

The metal substrate used was Q235 carbon steel (corresponding to ASTM A-36) sheet, with a size of $70 \times 15 \times 0.75$ mm. The applied coating was Type 881-Y01 acrylic polyurethane coating (produced by Beijing HCBM new material Co., Ltd., China).

The substrate surface was abraded manually with 120# abrasive paper and cleaned with ethanol and acetone in turn. The coating was brushed manually on the substrate. The coated samples were kept in air for a week at room temperature for sufficient curing. The coating thickness was measured with a TT220 thickness meter (Time Instruments Co. Ltd., China) and was 50 ± 5 μm .

Experimental Conditions

The coated samples were tested in following corrosive environments at room temperature:

- Complete immersion in 3.5% NaCl solution.
- Alternate wetting and drying condition: 4-h immersion in 3.5% NaCl solution and 8-hour drying in air in turn. One cycle was 12 h, denoted as 1C for convenience.

Measurement Methods

The coated samples were removed from the experimental environments for different exposure times, and electrochemical measurements were carried out in 3.5% NaCl solution at room temperature with a PARSTAT 2273 electrochemical system (Princeton Applied Research, USA). Electrochemical impedance spectra (EIS) were obtained at open circuit potential with a 10 mV sine perturbation. The measuring frequency range was

10^{-2} – 10^5 Hz. The exposed area of the working electrode was about 10.7 cm^2 . The reference electrode was a saturated calomel electrode (SCE). A Pt wire was coiled to use as a counter electrode and the area was about 15 cm^2 . Each test was repeated three times at least. ZSimpWin software was used to analyze the electrochemical impedance spectra in order to obtain the electrochemical parameters of the coatings.

Hitachi S4700 scanning electronic microscope (SEM) was used to observe the sample surface after different testing time. Nexus 8700 infrared spectrometer (Thermo Nexus 8700, USA) was used to analyze the structural changes in the coating after different testing time. The coating powders removed from the samples were pressed into thin pieces for FT-IR analysis. The window material was KBr. The spectral resolution was 4 cm^{-1} , and the number of the scans was 30.

Water absorptivity was estimated by coating capacitance according to Brasher-Kingsbury equation.¹⁵

$$X_v\% = 100 \times \log(C_c(t)/C_c(0)) / \log(80) \quad (1)$$

where $X_v\%$ is volume water absorptivity of coating, $C_c(0)$ and $C_c(t)$ are the capacitances of coating before and after immersion time t .

The porosity of the coating was calculated by coating resistance according to following equation.¹⁶

$$P = R_{pt} / R_p \quad (2)$$

where P is the coating porosity, R_p the pore resistance of coating obtained by EIS analysis, R_{pt} is the resistance supposed infinite coating porosity and is expressed as $R_{pt} = d/Ak$, in which k is the electrolyte conductivity (about 0.01 $\text{S} \times \text{m}$ for 3.5% NaCl solution at 25°C), A is the area of coating sample (about 10.7×10^{-4} m^2), and d is the thickness of coating (about 5×10^{-5} m).

RESULTS AND DISCUSSION

The EIS Spectra During Failure Process of the Coating Under Immersion or Alternate Wetting and Drying Condition

Figure 1 shows Nyquist plots of coating samples in 3.5% NaCl solution after testing under wet-dry cyclic condition and

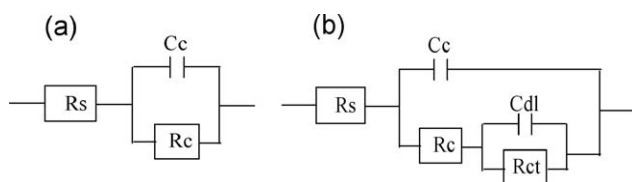


Figure 2. The equivalent circuits for the coating systems at different stages: (a) beginning and (b) middle and late stages.

immersion condition. It can be seen from Figure 1 that at initial stage, only a single semi-circle with high-impedance can be obviously observed, which may indicate that some water penetrated into the coating, but do not reach the coating/metal interface. The experimental data can be fitted by the equivalent circuit model (a) shown in Figure 2(a). In this circuit, R_S represents electrolyte resistance, C_C is the capacity of the coating, and R_p is the pore resistance of the coating. After testing for two circles (or 24 h), the second time constant can be observed in the Nyquist plot, and the capacitive loops at high frequency domain decreases obviously. These indicate that the electrolyte solution has partly penetrated through the coating and the metal substrate has been corroded. The experimental data can be fitted by the equivalent circuit model (b) shown in Figure 2(b), in which C_{dl} is the double-layer capacity and R_{ct} symbolizes the charge transfer resistance, associated with the kinetic of the corrosion process. But during the 2nd–4th circles, the evolutions of the impedance spectra of the coating samples for the two test conditions are different (Figure 1). Under wet-dry alternation from 2nd to 4th circle, with the test time increasing, the radius of capacitance loop at high frequency domain increases gradually [Figure 1(a)], indicating that the resistance of coating samples increased in a short time. However, under complete immersion condition from 24 to 48 h, with the test time increasing, the radius of capacitance loop at high frequency domain fluctuates very slightly [Figure 1(b)], implying a slight change of the resistance of the coating samples.

Figure 3 shows Nyquist plots of coating samples exposed to a wet-dry cyclic environment from 5th to 76th circles. In these Nyquist plots, the second time constant can also be observed,

implying that the electrolyte solution has partly penetrated through the coating and the metal substrate has been corroded. The experimental data can also be fitted by the equivalent circuit model (b) shown in Figure 2(b). From Figure 3(a), under wet-dry alternation from 5th to 11th circle, the radius of capacitance loop at high frequency domain increases gradually. However, from 24th to 76th circle, these values decrease obviously, indicating that an obvious decrease of the shielding properties of coatings.

The impedance of coated samples at low frequency (e.g. coating impedance at 0.01 Hz, simplified as $|Z|_{0.01\text{Hz}}$) can, to some extent, reflect the shielding property of coatings, and is widely used as a parameter to evaluate coating performance.¹⁷ Generally, the coatings with $|Z|_{0.01\text{Hz}}$ value above $10^8 \Omega \cdot \text{cm}^2$ can provide good protection, while those with $|Z|_{0.01\text{Hz}}$ value below $10^6 \Omega \cdot \text{cm}^2$ would provide poor protection.^{18,19} Figure 4 shows $|Z|_{0.01\text{Hz}}$ values of the coating system under two different testing conditions with testing time. At the beginning, the low frequency impedance $|Z|_{0.01\text{Hz}}$ of the coating was as high as $10^{11} \Omega \cdot \text{cm}^2$, indicating very good shielding property of the coatings. However, during the initial testing stage, the $|Z|_{0.01\text{Hz}}$ value of the coatings samples decreases quickly with time because of electrolyte permeation into the coating through micro-pores. With the time increasing further, for the coating samples exposed to the immersion environment, the $|Z|_{0.01\text{Hz}}$ value is not obviously changed for a long time (up to about 912 h). While for the coating samples exposed to the alternative wetting and drying environment, the $|Z|_{0.01\text{Hz}}$ value is not obviously changed for only about 264 h or 22 circles, and then decreases sharply during 22th to 34th circle, followed by an almost constant value up to about 912 h or 76 circles. Namely, the degradation of the coating exposed to a wet-dry alternation environment was more serious and quicker, implying that wet-dry alternation environment can accelerate the coating degradation.

In order to analyze the coating degradation, the EIS data are fitted by using the equivalent circuit model shown in Figure 2. Where, the coating capacity C_C is substituted by a constant phase angle element (CPE). Table I shows the capacity and pore resistance of the coating from the fitting results. The porosity and water absorptivity of the coatings can be calculated by the resistance and capacitance of coating obtained from fitting

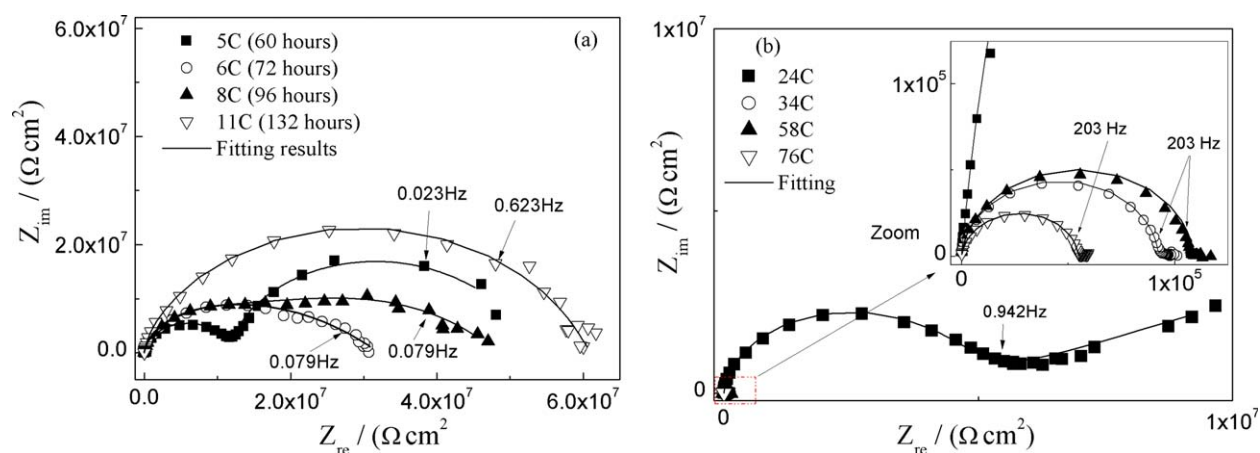


Figure 3. Nyquist plots of the coating samples exposed to wet-dry alternation environment (a) 5–11 cycles and (b) 22–76 cycles. [Color figure can be viewed in the online issue, which is available at wileyonlinelibrary.com.]

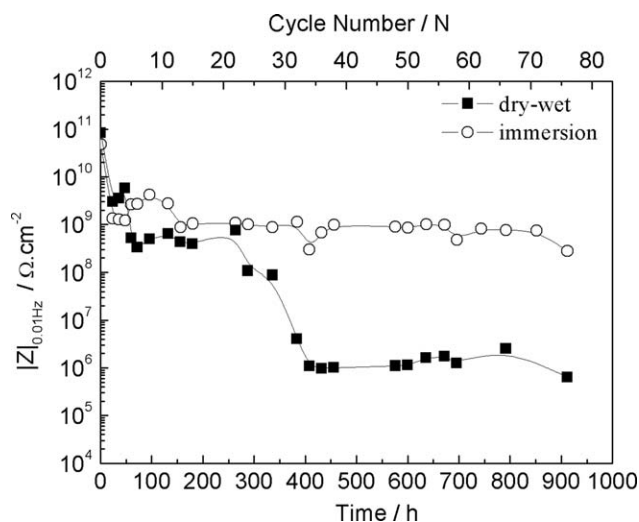


Figure 4. Changes of $|Z|_{0.01\text{Hz}}$ values of coating samples exposed to wet-dry and immersion environment with test time.

results of the EIS datum, respectively. Figure 5 shows the changes of the porosity and water absorptivity of the coatings exposed to wet-dry alternation and immersion conditions,

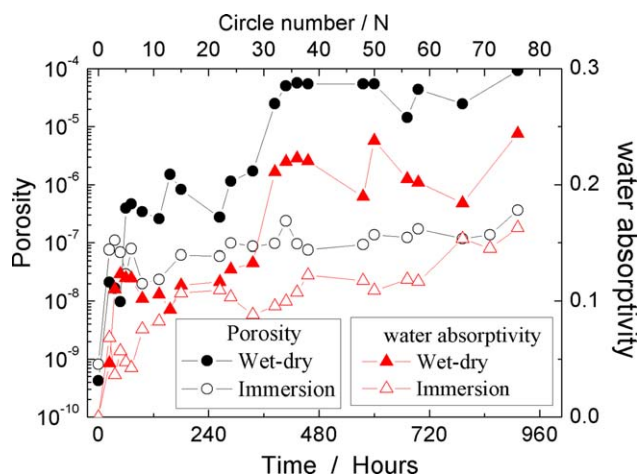


Figure 5. The changes of porosity and water absorptivity of coatings with time. [Color figure can be viewed in the online issue, which is available at wileyonlinelibrary.com.]

respectively. From Figure 5, it is clear that the porosity and water absorptivity of coatings under wet-dry alternation conditions are obviously greater than those under immersion condition.

Table I. The Capacity and Pore Resistance of the Coating from the Fitting Results

Time (hour)	R_p ($\Omega\cdot\text{cm}^2$)		CPE (n) ($\Omega/\text{cm}^2/\text{s}^n$)	
	Wet-dry	Immersion	Wet-dry	Immersion
Initial (about 0.5 h)	1.11E+10	5.75E+09	1.07E-09 (0.954)	1.67E-09 (0.960)
24 h (2C)	2.20E+08	6.15E+07	1.32E-09 (0.936)	2.25E-09 (0.929)
36 h (3C)	2.80E+08	4.28E+07	1.74E-09 (0.954)	1.95E-09 (0.957)
48 h (4C)	4.82E+08	6.82E+07	1.84E-09 (0.951)	2.14E-09 (0.949)
60 h (5C)	1.19E+07	1.61E+08	1.81E-09 (0.956)	2.05E-09 (0.953)
72 h (6C)	1.01E+07	5.93E+07	1.81E-09 (0.958)	2.01E-09 (0.957)
96 h (8C)	1.37E+07	2.34E+08	1.68E-09 (0.964)	2.32E-09 (0.934)
132 h (11C)	1.83E+07	1.99E+08	1.71E-09 (0.959)	2.39E-09 (0.943)
156 h (13C)	3.12E+06	-	1.61E-09 (0.966)	-
180 h (15C)	5.68E+06	7.54E+07	1.76E-09 (0.961)	2.66E-09 (0.936)
264 h (22C)	1.71E+07	7.92E+07	1.79E-09 (0.959)	2.69E-09 (0.947)
288 h (24C)	4.10E+06	4.78E+07	1.87E-09 (0.956)	2.62E-09 (0.940)
336 h (28C)	2.72E+06	5.42E+07	1.92E-09 (0.951)	2.45E-09 (0.944)
384 h (32C)	1.88E+05	4.81E+07	2.70E-09 (0.956)	2.53E-09 (0.943)
408 h (34C)	9.24E+04	1.98E+07	2.81E-09 (0.963)	2.58E-09 (0.941)
432 h (36C)	8.25E+04	4.88E+07	2.85E-09 (0.953)	2.67E-09 (0.939)
456 h (38C)	8.64E+04	6.20E+07	2.81E-09 (0.943)	2.85E-09 (0.932)
576 h (48C)	8.58E+04	5.07E+07	2.46E-09 (0.957)	2.79E-09 (0.936)
600 h (50C)	8.54E+04	3.42E+07	3.04E-09 (0.953)	2.69E-09 (0.941)
672 h (56C)	3.26E+05	3.84E+07	2.63E-09 (0.950)	2.80E-09 (0.939)
696 h (58C)	1.07E+05	2.72E+07	2.60E-09 (0.951)	2.78E-09 (0.940)
792 h (66C)	1.89E+05	3.98E+07	2.40E-09 (0.939)	3.26E-09 (0.911)
852 h (71C)	-	3.43E+07	-	3.15E-09 (0.933)
912 h (76C)	5.02E+04	1.29E+07	3.12E-09 (0.933)	3.40E-09 (0.929)

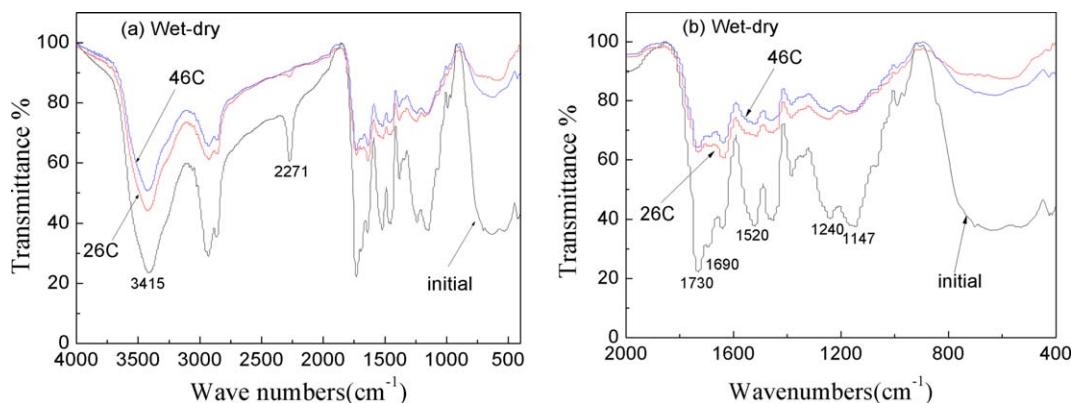


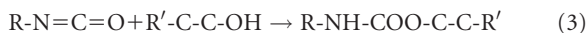
Figure 6. FT-IR spectra of acrylic polyurethane coatings samples for different times under wet-dry alternation condition (a) 4000–400 cm^{-1} ; (b) 2000–400 cm^{-1} . [Color figure can be viewed in the online issue, which is available at wileyonlinelibrary.com.]

The aforementioned results show that the failure rate of the coating under wet-dry alternation is faster than that under complete immersion.

The FT-IR Analysis on the Coatings

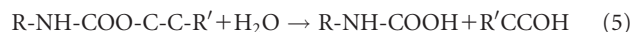
The changes of the functional groups of the acrylic polyurethane coating exposed to the wet-dry alternation condition with testing time were analyzed by FT-IR. Figure 6 shows the infrared spectra for the coating under wet-dry alternation condition. The absorption peak at 3415 cm^{-1} is attributed to the stretching vibration of the O—H bond. The —N=C=O stretching vibration peak is at 2275 cm^{-1} . The —C=O stretching vibration of acrylate group and the carbamate group in polyurethane peak are at 1730 cm^{-1} and 1690 cm^{-1} , respectively. The —N—H stretching vibration peak in the characteristic spectral band II of the sec-amide is at 1520 cm^{-1} , and the peaks at 1240 cm^{-1} and 1147 cm^{-1} are attributed to the infrared absorption band of —C—N. For the acrylic polyurethane paint, the hydroxyl groups of acrylic resin react with isocyanate groups (—N=C=O) for curing. The majorities of the hydrogen bonds are associative structures with different association strengths, showing the broad peak around 3415 cm^{-1} .

From Figure 6, it can be seen that after exposed to the wet-dry alternation environment, the —N=C=O absorption peak decreased significantly with testing time and eventually disappeared. The main reason may be attributed to that the isocyanate group (—N=C=O) in the coating can not only react with the hydroxyl group (—O—H) to cure further, but also hydrate with outer water, resulting in hydrolysis of the coating to generate CO_2 and further form pore defects.²⁰ The related equations are as follows:



It can also be found from Figure 6 that after the coating samples were tested under wet-dry alternation condition between the 26 and 46 cycles, the intensity of absorption peaks at 1730 cm^{-1} and 1690 cm^{-1} corresponding to carbonyl group decreased obviously because the C—O bonds of the —NHCOOR— molecular chains was broken partly. The —N—H stretching vibration peak at 1520 cm^{-1} reduced significantly, indicating that the fracture of the sec-amide group in acrylic polyurethane coating. In addition,

the absorption peak at 1240 cm^{-1} and 1147 cm^{-1} weakened due to the scission of —C—N bonds. Therefore, under a wet-dry alternate condition, the coating failure was accelerated because the chains of functional groups in the coating were broken, as shown in following equation.²¹



SEM Observation of the Coating Surface

Figure 7 shows the SEM morphologies of the coating surface exposed to wet-dry alternate environment with different times. It can be observed that after tested for 26 cycles, the coating surface became rough and porous. After 46 cycles, the coating surface got much rougher and some serious chalking appeared.

The Analysis of the Coating Failure Under Wet-Dry Alternation

The failure of organic coatings is a complicated process since it is affected by several factors such as coating type, defects, and the service environments. However, the water absorbability of the coatings may be one of the most important factors, because water in coatings may cause swelling or solvation of coatings, leading to the degradation of coatings. In addition, water affects the permeation of oxygen and other corrosive agents, and consequently the presence of such substances at coating-metal interface promotes corrosion of metal substrate. According to the aforementioned results, based on the wetting-drying model for water uptake and release proposed by Lendvay-Gyorik,¹² a failure process for acrylic polyurethane coating under a wet-dry cyclic condition can be suggested as following.

During the immersion stage under wet-dry alternate conditions, the coating absorbs water and ions in the electrolyte. The functional groups of the coating such as isocyanate group and ester group can all react with the water molecular, resulting in degradation of the coating,^{22–24} which is confirmed by above infrared spectra analysis. Moreover, the electrolyte can also penetrate into the coating through the pores and defects in the coating which are formed during curing and degrading. Corrosion will occur when the electrolyte reaches the metal substrate.

During the drying stage under the wet-dry alternate condition, the coating is to release water by evaporation into the air through the pores. The adhesive strength between the resins and

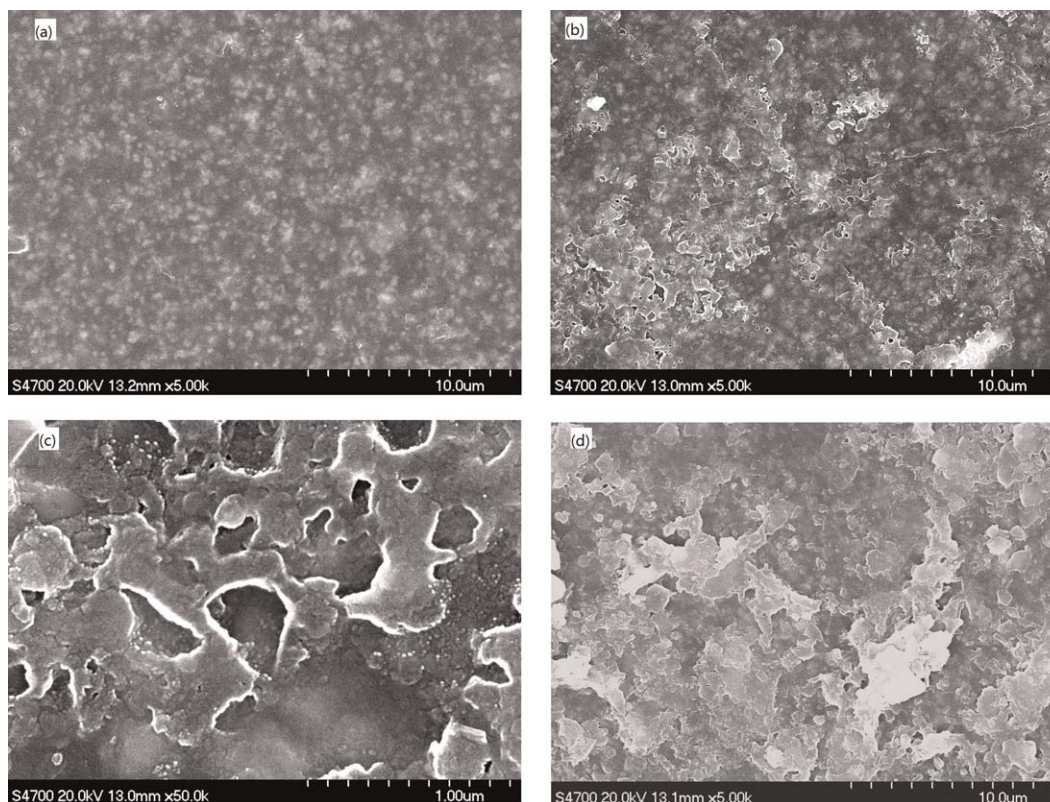


Figure 7. SEM morphology of the coating samples exposed to wet-dry alternate environment with different times (a) initial; (b) and (c) after 26 cycles; (d) after 46 cycles.

fillers in the coating decreases due to shrinking of the polymer resin. In addition, during the water release, oxygen from the air becomes easier to reach the substrate surface, which would accelerate the corrosion process.

Under the wet-dry alternate condition, the blistering failure of acrylic polyurethane coating can be supposed as following. The alternate water uptake and dehydration processes result in expansion and shrink of the coating volume, which causes the enlargement of the micro-pores in coating. During the immersion stage, the electrolyte permeated into the coating may aggregate in the micro-pores. While in the drying stage the aggregated electrolyte would in return permeate outward under the effect of the osmotic pressure, leading to the coating blistering and even cracking.²⁵ On the other hand, corrosion of the metal substrate can occur due to the electrolyte penetration through the pores in the wetting stage, and can be accelerated by increased oxygen reduction rate due to supplement of oxygen in the drying stage. As the testing time prolongs further, both the corrosion products produced beneath the coating and the strengthened oxygen reduction rate on the substrate surface would damage the bonding between the substrate and the coating,²⁶ which would cause more serious damages even exfoliation for the coating.

CONCLUSIONS

1. For the tested acrylic polyurethane coating, the failure rate under wet-dry alternation is obviously greater than that under complete immersion. Under wet-dry condition, both

the porosity and the water absorptivity of the coating are also greater than those under complete immersion condition.

2. Owing to the physical effect of wet-dry alternation, the fillers in the coating surface layer may fall off and result in micro-pores, which could multiply the defects in the coating and accelerate the coating degradation.
3. The isocyanate group in the coating not only participates in the curing of coating, but also hydrolyzes with water molecule. The C—O bonds fracture partly due to hydrolysis of the main molecule chains, which is one reason for the coating failure.

REFERENCES

1. Bierwagen, G. P. *Prog. Org. Coat.* **1987**, *15*, 179.
2. Fredj, N.; Cohendoz, S.; Mallarino, S.; Feaugas, X.; Touzain, S. *Prog. Org. Coat.* **2010**, *67*, 287.
3. Zhou, Q.; Wang, Y. *Prog. Org. Coat.* **2013**, *76*, 1674.
4. Deflorian, F.; Rossi, S. *Electrochim. Acta* **2006**, *51*, 1736.
5. Rezaei, F.; Sharif, F.; Sarabi, A. A.; Kasirih, S. M.; Rahmani, M.; Akbarinezhad, E. *J. Coat. Technol. Res.* **2010**, *7*, 209.
6. Fredj, N.; Cohendoz, S.; Feaugas, X.; Touzain, S. *Prog. Org. Coat.* **2010**, *69*, 82.
7. Zhu, Y.; Xiong, J.; Tang, Y.; Zuo, Y. *Prog. Org. Coat.* **2010**, *69*, 7.

8. He, S.; Xiong, J.; Tang, Y.; Zuo, Y. *J. Appl. Polym. Sci.* **2011**, *120*, 1892.
9. Park, J. H.; Lee, G. D.; Ooshige, H.; Nishikata, A.; Tsuru, T. *Corros. Sci.* **2003**, *45*, 1881.
10. Coniglio, N.; Nguyen, K.; Kurji, R.; Gamboa, E. *Prog. Org. Coat.* **2013**, *76*, 1168.
11. Zhao, X.; Wang, J.; Wang, Y.; Kong, T.; Zhong, L.; Zhang, W. *Electrochem. Commun.* **2007**, *9*, 1394.
12. Lendvay-Gyorik, G.; Pajkossy, T.; Lengyel, B. *Prog. Org. Coat.* **2006**, *56*, 304.
13. Allahar, K. N.; Hinderliter, B. R.; Bierwagen, G. P.; Tallman, D. E.; Croll, S. G. *Prog. Org. Coat.* **2008**, *62*, 87.
14. Zhang, W.; Chen, X.; Yin, P.; Xu, Z.; Han, B.; Wang, J. *Appl. Mech. Mater.* **2011**, *161*, 58.
15. Brasher, D. M.; Kingsbury, A. H. *J. Appl. Chem.* **1954**, *4*, 62.
16. Armstrong, R.; Wright, J. *Electrochim. Acta* **1993**, *38*, 1799.
17. Bierwagen, G.; Tallman, D.; Li, J. P.; He, L. Y.; Jeffcoate, C. *Prog. Org. Coat.* **2003**, *46*, 148.
18. McIntyre, J. M.; Pham, H. Q. *Prog. Org. Coat.* **1996**, *27*, 201.
19. Bierwagen, G. P.; He, L.; Li, J.; Ellingson, L.; Tallman, D. E. *Prog. Org. Coat.* **2000**, *39*, 67.
20. Liu, D. Methods and procedure for failure analysis of coatings; Chemical Industry Press: Beijing, 1st ed., **2003**, pp. 125–132 (in Chinese).
21. Ni, X.; Li, X.; Zhang, S.; Qiu, D. J. *Wuhan Univ. Technol.* **2009**, *24*, 892.
22. Perrin, F. X.; Irigoyen, M.; Aragon, E.; Vernet, J. L. *Polym. Degrad. Stab.* **2000**, *70*, 469.
23. Schoonovera, J. R.; Thompson, D. G.; Osborn, J. C.; Bruce Orler, E.; Wroblewski, D. A.; Marsh, A. L.; Wang, H.; Palmer, R. A. *Polym. Degrad. Stab.* **2001**, *74*, 87.
24. SchuÈtz, E.; Berger, F.; Dirckx, O.; Chambaudet, A. *Polym. Degrad. Stab.* **1999**, *65*, 123.
25. Yang, X.; Vang, C.; Tallman, D. E. *Polym. Degrad. Stab.* **2001**, *74*, 341.
26. Furbeth, W.; Stratmann, M. *Corros. Sci.* **2001**, *43*, 207.